**Atmospheric
Chemistry
and Physics
Discussions**

A numerical
modelling study on
regional mercury
budget

X. Lin and Y. Tao

Title Page

Abstract   Introduction

Conclusions   References

Tables   Figures

⏮   ⏭

◄   ►

Back   Close

Full Screen / Esc

Print Version

Interactive Discussion

© EGU 2003

A numerical modelling study on regional mercury budget for eastern North America

X. Lin[1] and Y. Tao[1]

[1]Kinectrics, 800 Kipling Avenue, Toronto, M8Z 6C4, Canada

Correspondence to: X. Lin (xiude.lin@kinetrics.com)

Abstract

In this study, we have integrated an up-to-date physio-chemical transformation mechanism of Hg into the framework of US EPA's CMAQ model system. In addition, the model adapted detailed calculations of the air-surface exchange for Hg to properly describe
Hg re-emissions and dry deposition from and to natural surfaces. The mechanism covers Hg in three categories, elemental Hg (Hg^0), reactive gaseous Hg (RGM) and particulate Hg (HgP). With interfacing to MM5 (meteorology processor) and SMOKE (emission processor), we applied the model to a 4-week period in June/July 1995 on a domain covering most of eastern North America. Results indicate that the model
simulates reasonably well the levels of total gaseous Hg (TGM) and the specific Hg wet deposition measurements made by the Hg deposition network (MDN). Moreover, results from various scenario runs reveal that the Hg system behaves in a closely linear way in terms of contributions from different source categories, i.e. anthropogenic emissions, natural re-emissions and background. Analyses of the scenario results suggest
that 37% of anthropogenically emitted Hg was deposited back in the model domain with 5155.2 kg of anthropogenic Hg moving out of the domain during the simulation period. Overall, the domain served as a source, which supplied a net 461.2 kg of Hg to the global background pool over the period. Our model validation and a sensitivity test further rationalized the rate constant for gaseous oxidation of Hg^0 by hydroxyl
radical OH used in the global scale modelling study by Bergan and Rodhe (2001). A further laboratory determination of the reaction rate constant, including its temperature dependence, stands as one of the important issues critical to improving our knowledge on the budget and cycling of Hg.

1. Introduction

Atmospheric Mercury (Hg) exists primarily in inorganic forms with three states, i.e. Hg^0 (elemental Hg), RGM (reactive gaseous divalent Hg) and HgP (particulate Hg). Al-

A numerical modelling study on regional mercury budget

X. Lin and Y. Tao

though the existence of methylated Hg has been reported, it only accounts for less than 3% of the total gaseous Hg, except areas near emissions sources. On the other hand, monovalent Hg (Hg^+) is unstable in the atmosphere. Under normal atmospheric conditions, Hg^0 is the main component of gaseous Hg, and constitutes the majority of Hg in the atmosphere. RGM is readily dissolved into the water. Subsequently, it is involved in aqueous phase reactions, and is also subject to adsorption onto the elemental carbon aerosols. HgP is referred to as particulate solid Hg, which can exist in both gaseous phase and aqueous phase. Now, it is well known that atmospheric Hg, predominantly in the gaseous elemental form, has a global atmospheric residence time of about a year. Such a time scale leads to significant long-range transport of the atmospheric Hg and its deposition in the areas distant from major point sources (Fitzgerald et al., 1998). Numeric modelling stands as a useful tool to study the complex chemical transformation, transport and deposition processes of atmospheric Hg.

Hg is released into the atmosphere from both anthropogenic and natural sources. While anthropogenic Hg is mainly contributed by chloral-alkali production, coal combustion and waste incineration, natural sources of Hg are volcanoes, soils, forests, lakes, rivers and oceans. It was estimated that about 5500 mg of Hg were emitted globally in 1995 (U.S. EPA, 1997). Recent studies have indicated that Hg re-emitted from various natural surfaces represents a very important part in the atmospheric Hg burden. Mason et al. (1994) suggested a global marine emission of 2000 mg year^{-1}. Lindberg et al. (1998) estimated an annual emission of 1400 to 3200 mg of Hg attributable to terrestrial origins (forests and soils). Apparently, in order to gain more accurate insight into the Hg budget and, thereafter, to design suitable abatement strategies, it is imperative to place anthropogenic emissions into a proper perspective. In this context, modelling studies on a regional scale need to appropriately include the important component of Hg emissions from natural surfaces.

To study the transport and deposition of the atmospheric Hg in Europe and the United States, several regional modelling studies have been carried out. While employing the anthropogenic emission inventories and providing valuable information on Hg chem-
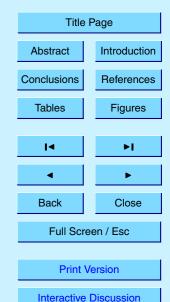
istry, transport and deposition, some studies did not include detailed descriptions on the re-emissions of Hg from natural surfaces. In general, the natural re-emissions were either included in the global background (Bullock et al., 1997; Bullock, 2000; Petersen et al., 1998, 2001; Seigneur et al., 2001) or highly parameterized by a latitude and sea-

5 son dependence (Shannon and Voldner, 1995). Recently, Xu et al. (2000) integrated a Hg component into the Sarmap Air Quality Model (SAQM) (Chang et al., 1996). In their work, a parameterized Hg mechanism similar to the one of Petersen et al. (1995) was adopted. However, significant improvement was made in the estimation of re-emissions of Hg from natural surfaces. Exchanges of Hg between air and the earth

10 surface were explicitly calculated to depict its emissions and dry deposition from and to the surfaces. Most recently, Bullock and Brehme (2002) developed a regional Hg model based on the framework of a state-of-the science regional air quality model, the US EPA's Community Multi-scale Air Quality (CMAQ) model (Byun and Ching, 1999). In their model, a detailed physio-chemical mechanism of Hg involving both gaseous

15 and aqueous phases was included to provide a more accurate description of the atmospheric Hg in three states (Hg^0, RGM and HgP). Again, pre-determined boundary conditions were used to represent the contributions to the atmospheric Hg burden from both global background and natural emissions that originated within the model domain. In the present study, we have further advanced their work by integrating a set of treat-

20 ments for the atmosphere- surface exchange of Hg. The modelling system was applied to a domain covering most of eastern North America. This paper describes our model structure, a preliminary validation of the model, a quantitative estimation of regional Hg budget and an investigation on the reaction rate constant of the important gaseous oxidation of Hg by hydroxyl radical OH and its impact on the atmospheric Hg modelling

25 practice.

X. Lin and Y. Tao

Print Version

Interactive Discussion

2. Hg Mechanism integrated into the CMAQ model system

CMAQ is an advanced regional air quality modelling system. It was developed by the Atmospheric Modeling Division of the U.S. EPA (Byun and Ching, 1999) to simulate the transport, chemical transformation and deposition of air pollutants. Built on a "one-atmosphere" approach, CMAQ is so comprehensive in scope that it allows for the simulation of acid deposition, O3 and photochemical oxidants, and fine/coarse particulate matter at spatial scales ranging from urban to regional. CMAQ can be constructed within a computational framework, named Models-3. The framework enables users to interact with the modelling system through a high-level graphical user interface. Through the graphics and visualization capabilities, the framework facilitates data transmission among the components of the system and analysis of model simulation results. However, CMAQ, like its emission preprocessor SMOKE, can also be run in a stand-alone mode by executing scripts, which comprise various UNIX shell commands. In our present study, the stand-alone CMAQ version of June 2001 is utilized as an integration platform. Among the options supported by CMAQ in gaseous phase chemical mechanisms and numerical chemistry solvers, we selected RADM2 as the chemical mechanism and the QSSA solver to solve the stiff chemical system. Further, a physio-chemical transformation mechanism of Hg is integrated into the platform.

The physio-chemical transformation mechanism of Hg integrated into the CMAQ model is presented in Table 1. It is generally similar to the one used by Bullock and Brehme (2002). The mechanism involves Hg in three categories, Hg^0, RGM and HgP. Some differences from Bullock and Brehme (2002) in the detailed treatment of the mechanism exist and are worthy to be noted as follows.

1. We assume that particulate mercury consists of two components, a soluble one and an insoluble one. The co-existence of the two HgP components in the atmosphere is rationalized by the Hg sorption experiments (Seigneur et al., 1998).

2. Products of gaseous oxidation reactions of $Hg^0_{(g)}$ with O_3/OH are allocated into two parts, 50% in RGM and 50% in insoluble HgP. The division of the reaction prod-

ucts was based on the study by Hall (1995) and the recommendation of Travnikov and Ryaboshapko (2002).

3. A reaction rate constant of 8.7×10^{-14} cm^3 molec^{-1} s^{-1} for Hg$^0_{(g)}$ oxidation by hydroxyl radical OH was originally reported by Sommar et al. (2001). This rate constant together with a normal OH levels would lead to a Hg^0 lifetime of about 4–7 months. It should be noted that this rate has not been confirmed independently by any other laboratories yet. Travnikov and Ryaboshapko (2002) cautioned the high rate value. Ryaboshapko et al (2002) suggested a further investigation on the rate constant. More significantly, Bergan and Rodhe (2001) used a global model to evaluate the potential role of the oxidation reactions of Hg^0. They found that the oxidation rate of Sommar et al. (2001) is too large (by about a factor of 3) to reconcile the model calculations with the observed global distribution of Hg^0 and divalent Hg. Based on their findings, we set the rate constant at 2.9×10^{-14} cm^3 molec^{-1} s^{-1} in the present study. Later on, a sensitivity test on the reaction rate constant will be conducted and discussed in Sect. 5.

4. In addition to its production from the oxidation in gas phase, insoluble HgP is also emitted from anthropogenic sources. Dissolved RGM in cloud water is subject to adsorption onto the atmospheric particulate matter. The adsorption leads to the generation of soluble HgP that, subsequently, is subject to a desorption process. The resultant sorption equilibrium is represented by an adsorption coefficient ($k = 34$ L g^{-1}) and an average particulate matter concentration in the cloud droplet of 0.02 g L^{-1} as recommended by Seigneur et al. (2001).

5. Based on Seigneur et al. (2001), Cl$_2$ is set to 10 ppt during the day; and 100 and 50 ppt for the first layer and the layers above, respectively, at night over the ocean. As for the inland, a zero concentration is assumed. A concentration of Cl$^-$ in the cloud water of 1.0×10^{-3} g L^{-1} is adopted from Bullock and Brehme (2002).
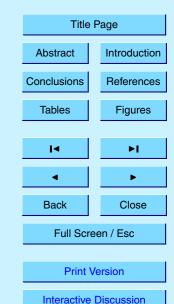
It is worth noting that the dry deposition of Hg^0 was omitted in Bullock and Brehme (2002). The modelling study by Xu et al. (2000) suggested that the dry deposition

of Hg^0 could account for about 20% of the total Hg deposition. In the present study, we calculated the dry deposition velocity for Hg^0 using a detailed treatment on the air-surface exchange of Hg^0 as described in Sect. 4.

3. Anthropogenic emissions of Hg

The model domain is shown in Fig. 1. Horizontally, the domain covers most of eastern North America and contains 78 × 67 grids with a grid spacing of 36 km. Vertically, it has 15 layers with varying thickness defined in the σ-coordinates and is stretching from the surface to about 15 000 m above the ground. The anthropogenic emissions of Hg input to the model were compiled using SMOKE (version 1.4B). Two 1995 inventories, the US one and the Canadian one, were utilized in the compilation. The US inventory, acquired from US EPA, cover all three species of Hg for point, area and mobile sources. On the other hand, the Canadian Hg emissions inventory, provided by Environment Canada, only includes the emissions for total Hg from point sources. To speciate the total Hg into its three species, we assumed different partitions for different industrial sectors following the treatment of Seigneur et al. (2001). More specifically, 56/42/2 of the Hg^0/RGM/HgP partition was set for coal-fueled electric utilities; 95/5/0 for chlor-alkali facilities; 85/10/5 for iron-steel industry; 100/0/0 for mining industry; and 50/30/20 for chemical manufacturing industry. The last ratio also served as the default for any sources that were out of the 5 industry categories.

As for the Canadian area and mobile sources of Hg, Environment Canada has pre-compiled a regional inventory for a 50 km × 50 km grid domain. The Canadian area and mobile emissions were mapped onto the defined model domain. A 50/30/20 partition among the three Hg species was assumed. SMOKE was used to process US area sources, US mobile sources and US/Canada point sources for Hg. These processed anthropogenic Hg emissions were finally integrated together with the output from normal SMOKE runs for the conventional RADM2 species and the Hg^0 re-emissions from natural surfaces generated from the process as described in Sect. 4. The integration

resulted in netCDF-formatted emission files for inputting to CCTM (**C**MAQ's **c**hemical **t**ransport **m**odel, the core model of CMAQ system).

4. Re-emissions and dry deposition of Hg^0 from and to natural surfaces

In the present study, we adopted the general approaches of Xu et al. (1999) to calculate
5   the mass transfer (emissions and dry deposition) of Hg^0 caused by the air-surface ex-
changes. Briefly, the Penman-Monteith equation for evaportranspiration rate (Monteith
and Unsworth, 1990) was employed in dealing with Hg^0 emissions from plant canopies.
An empirical relationship between the net Hg^0 flux at the air-soil interface and soil tem-
perature by Carpi and Lindberg (1998), calibrated by excluding the deposition flux, was
10 used to estimate the emissions from soils. To calculate the emissions from water, an
assumption, that the overall mass transfer coefficient of Hg^0 at the air-water interface
can be approximated by its mass transfer coefficient in the water, was made. In our
view, this assumption can be further rationalized by applying Liss and Slater (1974)'s
two-layer model to the interface and is supported by the data provided in Shannon and
15 Voldner (1995) and Poissant et al. (2000).

To facilitate the evaluation of the mass transfer (emissions and dry deposition) of
Hg^0, we modified MCIP, the **m**eteorology **c**hemistry **i**nterface **p**rocessor of the CMAQ
modelling system, by integrating the algorithms of air-surface Hg^0 exchanges. The
modified MCIP generated natural re-emissions and dry deposition velocity of Hg^0. One
20 of MCIP's original output files, METCRO2D, was expanded to include this additional
information. As being input to CCTM runs, the file was also used to generate the
netCDF-formatted emission input files as described in Sect. 3.

It is worth noting that there are two main differences from Xu et al. (1999) in calcu-
lations of Hg^0 fluxes. The first is related to the quantification of Hg^0 content in surface
25 soil water. To compute the emissions from the plant canopies using the evaportran-
spiration rate, the Hg^0 concentrations in the surface soil water need to be defined. Xu
et al. (1999) set a "universal" soil water Hg^0 concentration such that it had a value of

A numerical modelling study on regional mercury budget

X. Lin and Y. Tao

Title Page

Abstract	Introduction
Conclusions	References
Tables	Figures

◄   ►►

◄   ►

Back   Close

Full Screen / Esc

Print Version

Interactive Discussion

© EGU 2003

100 ng l^{-1} for a minimum water stress case. To provide more reasonable geographical variations for the Hg^0 concentration, we linked the soil contamination to the deposition of Hg. Because of relatively short lifetimes of RGM and HgP compared to Hg^0, we assumed that, as an approximation at the first order, the Hg^0 content in surface soil water at a concerned location would be proportional to the product between the strength of a contributing anthropogenic RGM/HgP source and the squared reciprocal of the distance between the contributing source and the concerned location.

A geographical distribution of the summed product was then generated by adding the contributions from all anthropogenic RGM and HgP sources within the modelling domain for each grid of the domain. According to the field study of Poissant and Casimir (1998), the Hg contents in surface soil water in southern Quebec, as derived from measured fluxes of Hg and water vapour, were about 15 ng L^{-1}. This value was used to calibrate the summed variables to create a geographical distribution of Hg^0 content in surface soil water for the modelling domain. The resultant distribution gives 70 ng L^{-1} of Hg^0 in soil water for east-central Tennessee. This level is adequate to explain the observed emission rates from plant canopies (Lindberg et al., 1998).

The second difference lies in the estimation of the mass transfer coefficient of Hg^0, K_w, in water when calculating the air-water exchanges. While Xu et al. (1999) used empirical formulae of Mackay and Yeun (1983) and Asher and Wanninkhof (1995), we adopted the approach by Poissant et al. (2000). Briefly, K_w (cm h^{-1}) can be correlated with the mass transfer of CO_2 across the airwater interface through (Wanninkhof et al. 1985, Hornbuckle et al., 1994)

$$K_w = (0.45U_{10}^{1.64})[Sc_w(Hg^0)/Sc_w(CO_2)]^{-0.5},$$

where U_{10} is the wind speed (m s^{-1}) at 10 m and Sc's are the Schmidt numbers for CO_2 and Hg^0 in water, respectively. The Schmidt number of CO_2 is calculated using the temperature-corrected dependency (Hornbuckle et al., 1994; Bidleman and McConnell, 1995)
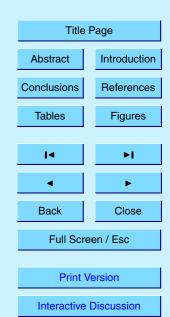
$$Sc_w(CO_2) = 0.11\,T^2 - 6.16\,T + 644.7$$

with T in °C. The Schmidt number of Hg^0 is directly derived from its definition

$$SC = v/D,$$

where the temperature (°C) dependant v (kinematic viscosity of water, $cm^2\ s^{-1}$) and D (diffusivity of Hg^0 in water, $cm^2 s^{-1}$) are estimated by

$$v = 0.017 \exp(-0.025\,T) \qquad \text{(Thibodeaux, 1996)},$$

$$D = 6.0 \times 10^{-7}\,T + 10^{-5} \qquad \text{(Kim and Fitzgerald, 1986)}.$$

The re-emissions of Hg^0 in the model domain accumulated over a 4-week period from 20 June 1995 to 18 July 1995 are presented in Fig. 2. It is seen that the re-emissions substantially diminish in the northern part of the model domain. This is partially due to minimized agricultural coverage in the regions. As Xu et al. (1999) indicates, re-emissions from agriculture are significantly larger than the re-emissions from forest and other land-use categories. The land-use effect is further enhanced by a less mercury content in surface soil water owing to much less anthropogenic sources than in the southern regions. In the eastern part of the model domain, relatively high re-emissions over the Atlantic Ocean coincide with higher average wind speed (not shown here). It is the high wind speed that causes the relatively high re-emissions through the wind dependence of the air-water exchange stated above.
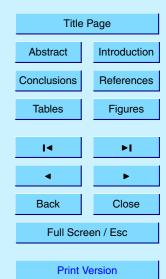
5. Model runs, results and discussion

In the study, we carried out the regional Hg modelling for the time period of 16 June 1995 to 18 July 1995. The modelling procedure started with a normal run of the meteorological processor MM5, a modified MCIP run and a normal run of the emission processor SMOKE. Then, a second SMOKE run with Hg emission inventories was conducted before executing the modified CCTM for Hg. To account for the global background of Hg, we set boundary conditions of 0.2 ppt for Hg^0, $0.01\,ng\,m^{-3}$ for both

RGM and HgP. These background levels are similar to the ones chosen by Bullock and Brehme (2002) and Xu et al. (2000). The same values were assigned for Hg initial conditions. Although our model runs covered a 32-day period, the results from the first 4 days were excluded from analysis to avoid the unstable data in the initial "warm-up"
5 period of a normal numerical modelling practice. To facilitate analysis, we conducted runs for 4 different scenarios. The 4 scenarios are

1. S_0, a base-line scenario, which includes both anthropogenic emissions and re-emissions of Hg from natural surfaces as well as Hg boundary conditions;

2. S_{ba}, the same as S_0 but without re-emissions of Hg from natural surfaces;

10 3. S_{bn}, the same as S_0 but without anthropogenic emissions of Hg; and

4. S_b, the same as S_0 but without both anthropogenic emissions and re-emissions of Hg from natural surfaces.

5.1. Model validation

To have a preliminary evaluation of the regional Hg model, we compared the model
15 results from the S_0 run with the measured ground level concentrations of total gaseous Hg (TGM) (Fitzgerald et al., 1991; Burke et al., 1995; Lindberg and Stratton, 1998; Blanchard et al., 2002) and Hg wet deposition at the sites of Hg deposition network (MDN) (Lindberg and Vermette, 1995; http://nadp.sws.uiuc.edu/nadpdata/mdnsites. asp). The measurement sites are plotted in Fig. 1 together with the model domain.
20 While the TGM measurements represented general long-term averaged values, the MDN's data used in the study were those taken from June–July of 1995. Since our model runs covered a period from 20 June 1995 to 18 July 1995 after excluding the "warm-up" period of model initiation, we can make a direct comparison between the modelled wet deposition of Hg and the MDN data.
25 For an illustration purpose, we plotted the total wet deposition of Hg over the 4-week period calculated from the S_0 run in Fig. 3. In parallel, the total precipitation

over the same period, which was derived from MM5 runs and was input into CMAQ, is plotted in Fig. 4. While the two variable fields show similar distribution patterns, some differences in the intensity exist in the east coastal and some central US regions. This disparity can be explained by the distribution of anthropogenic emission sources.

5 It is known that the majority of Hg wet deposition are attributable to RGM and HgP and that the concentrations of RGM and HgP peak in the vicinities of the sources due to their relatively short lifetime. Therefore strengthened anthropogenic emissions in these regions, as shown in Fig. 5, compensated the relatively small precipitation and eventually led to significant wet deposition.

10 Table 2 presents the comparisons of our model results from the scenario S_0 run with the field measurements. For ground level concentrations of TGM, the model results including both Hg^0 and RGM were averaged over the modelling period. It is seen that the averaged TGMs derived from the model agree well with the measurements. In general, the modelled results are within 10% of the observations. As for the wet deposition

15 of Hg, six MDN sites reported valid total wet deposition of Hg for the entire 4-week modelling period. As shown in Table 2, the model did reasonably well in simulating the measured total wet deposition. The relative simulation errors lie between −26% and +45%. Since MDN sites were usually measuring the Hg wet deposition on a weekly basis, analysis was also conducted for the weekly data. Among all MDN sites, there

20 are 35 valid weekly deposition data involving 11 sites during the 4-week period. The weekly data of the 11 sites are listed in Table 3 together with their modelled counterparts. A scatter plot with a least-squares regression line and a forced regression line with zero intercept is presented in Fig. 6. This plot is indeed parallel to Fig. 5b of Bullock and Brehme (2002). The present calculated correlation coefficient is 0.46, indicating

25 an improvement over the correlation coefficient 0.329 by Bullock and Brehme (2002). More comparisons of statistics are summarized in Table 4. While Bullock and Brehme (2002) significantly over-predicted the mean value and the variability of the measured data, the present study improved the two statistics with a slight over-estimation of 5.2% and a slight under-estimation of 2.6%, respectively. The improvement is reflected in all

A numerical modelling study on regional mercury budget

X. Lin and Y. Tao

Title Page

Abstract | Introduction

Conclusions | References

Tables | Figures

◀ | ▶

◀ | ▶

Back | Close

Full Screen / Esc

Print Version

Interactive Discussion

4 quartiles.

The moderate improvement mainly resulted from the reduced rate constant of the gaseous oxidation of Hg^0 by OH. As to be shown in a sensitivity analysis below, a reduction of the rate constant by two third of the value originally reported by Sommar et al. (2001) leads to a significant decrease of $\sim$5000 kg in the total wet deposition over the simulation domain for the entire modelling period. At the same time, as a regional budget analysis in the next section indicates, this decrease is compensated by a small increase (180.3 kg) in the wet deposition due to the inclusion of the re-emissions from natural surfaces.
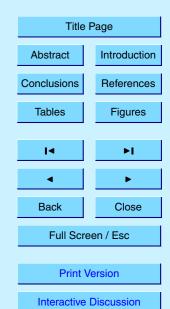
5.2. Regional budget

To investigate the regional budget of Hg, we calculated the domain total deposition of Hg over the modelling period of 20 June 1995 to 18 July 1995. The calculations were done for each of the 4 scenarios defined above. The resultant total deposition for all three components of Hg is presented in Table 5. The deposition was further segregated into the dry part and the wet part. Also shown in the table are total emissions released from the sources within the model domain during the simulation period. From the table, re-emissions of Hg from natural surfaces account for 60% of total Hg emissions or 1.5 times of anthropogenic Hg emissions. It is of interest to note that the Hg system behaves in a nearly linear way. Based on the four scenario definitions, the close linearity can be illustrated by comparing the summed value of S_0 and S_b with the summed value of S_{ba} and S_{bn} for each of the deposition categories in Table 5. By subtracting the value of a variable in S_b from its counterpart in another scenario, we estimated contribution to the variable from an emission component, which was added onto the S_b to form the other scenario. More specifically, we calculated the contributions to dry/wet deposition from anthropogenic emissions plus natural re-emissions, anthropogenic emissions only and natural re-emissions only, respectively. The estimated values are listed in the brackets in Table 5. From the table, one may observe the followings.

1. Among 8216.4 kg of Hg emitted anthropogenically, 3061.2 kg (37.3%) were directly deposited back in the domain. Accordingly, 62.7% of anthropogenic Hg (5155.2 kg) moved out of the domain and, subsequently were integrated into the background. This partition is similar to U.S. EPA (1997).

2. Among 12480.9 kg of naturally re-emitted Hg, 704.0 kg (5.6%) were directly deposited back in the domain with 180.3 kg deposited though the wet process. A majority part (94.4%) of the re-emitted Hg moved out of the domain and was integrated into the background.

3. The background contributed 16477.0 kg of Hg deposition in the domain, accounting for 81.4% of total deposition.

4. While background contributions predominated, anthropogenic emissions contributed more than 5 and 7 times than the re-emissions to the dry deposition and the wet deposition, respectively.

5. While a total of 20697.2 kg of Hg was emitted, 20236.0 kg of Hg were received by the surface within the domain through deposition processes. This resulted in a net loss of 461.2 kg and, therefore, indicates the domain as a whole acting as a net supplier to the background pool of Hg for the 4-week simulation period. The net contribution to the background pool only accounts for about 2% of the amount of Hg received in the domain. Considering the approximately equal weighting between the wet deposition and the dry deposition, the sign of the relatively small net contribution could be changed if precipitation fields during the modelling period were altered.

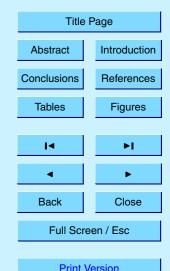5.3.   Sensitivity of rate constant of gaseous oxidation by OH

As mentioned previously, in their global modelling study, Bergan and Rodhe (2001) found that the rate constant of gaseous oxidation by OH of Sommar et al. (2001) is too large by about a factor of 3 to simulate the observed global distribution of Hg^0

and divalent Hg. Based on their findings, we set the rate constant at 2.9×10^{-14} cm^3 molec^{-1} s^{-1} in the study. To shed light upon the impact of the rate constant on the model simulations, we reset the rate at 8.7×10^{-14} cm^3 molec^{-1} s^{-1} and run the CCTM with emissions, initial/boundary conditions and all other inputs kept at the same val-

5　ues as Scenario S_0. Results indicated that the fast oxidation reactions led to more production of RGM and HgP. Consequently, more dry and wet deposition was generated at the expense of Hg^0. Over the entire modelling period, the domain total dry and wet depositions were 12068.0 kg and 14960.4 Kg, respectively. These numbers represent a 15.9% increase of the dry deposition and a 53.7% increase of the wet de-

10　position. Accordingly, the domain averaged ground level concentration of TGM dropped by 0.054 ng/m^3 (3.2%) from the S_0's value. Under this circumstance, the domain would serve as a strong sink in the sense of a global budget with a net gain of 6331.2 kg of Hg. This net gain would be equivalent to 30.6% of the amount emitted both anthropogenically and from natural surfaces within the domain. Evidently, such a large

15　positive percentage is not consistent with the human and industrial activities within the region in a global context.

　　The model results from the sensitivity test run were also compared against the measurements. The calculated ground level concentrations of TGM for the 6 observation sites were 0.04–0.08 ng/m^3 less than their counterparts from the S_0 run. The drops in

20　such a range did not practically weaken the model performance for TGM. The simulation of the wet deposition measurement, however, was significantly deteriorated. To illustrate the deterioration, we calculated bias, error, relative bias, relative error, root mean squared error (RMSE) and index of agreement (IOA) for model results from both the S_0 run and the sensitivity test run. While bias, error, relative bias, relative error and

25　RMSE follow their conventional definitions; IOA is defined as

$$IOA = 1 - \frac{N(RMSE)^2}{\sum\limits_{i=1}^{N}(|M_{i'}| + |O_{i'}|)^2},$$

where N is the total number of samples, $M_{i'}$ and $O_{i'}$ are the departures from the mean observed value of the modelled value and the observed value, respectively. A value of IOA = 1 indicates a perfect agreement and IOA = 0 indicates absolutely no agreement (Hedley et al., 1995). Calculated statistics are shown in Table 6. It is seen that the tripled rate constant caused much higher wet deposition of Hg at the MDN sites and worse agreement with the measurements than the S_0 run. As shown by the values of bias, the mean value of the 35 samples would be 262.5 ng/m^2 higher than the measured mean compared to 20.4 ng/m^2 higher in the S_0 case. This over-prediction is even larger than the overestimation of 234.4 ng/m^2 by Bullock and Brehme (2002) (as seen in Table 4), apparently due to the inclusion of the Hg re-emissions from natural surfaces in the study.

6. Conclusions

In the present study, we integrated an up-to-date physio-chemical transformation mechanism of Hg and detailed calculations on the air-surface exchange of Hg^0 into the framework of US EPA's CMAQ model system. An application of the constructed Hg model to a 4-week period in June/July 1995 indicated that the comprehensive model simulated reasonably well the specific wet deposition measurements of Hg at the MDN sites as well as the general ground level concentrations of TGM. Results from various scenario runs revealed that the Hg system behaves in a closely linear way in terms of the source contributors, i.e. anthropogenic emissions, natural re-emissions and background. Analyses on model results showed that 37% of anthropogenically emitted Hg were deposited back in the model domain with 63% (5155.2 kg) of anthropogenic Hg moving out of the domain during the simulation period. Overall, the domain served as a source to supply a net of 461.2 kg of Hg into the global background pool over the simulation period. This amount represents about 2% of the Hg amount received by the surfaces in the domain.

It should be noted that the present study is subject to limitations or uncertainties as

A numerical modelling study on regional mercury budget

X. Lin and Y. Tao

any similar modelling studies. These limitations or uncertainties are ranged widely from emissions, meteorology prediction, mechanism description, and deposition treatment to lack of dry deposition comparison. Following other significant pioneer works, we carried out this comprehensive regional modelling study by including the up-to-date physio-chemical transformation mechanism of Hg and the up-to-date treatment of Hg re-emission and dry deposition. Through the model validation and a sensitivity test, it emerges that the currently reported reaction rate constant of the gaseous oxidation of Hg^0 by hydroxyl radical OH could be too large by a factor of 3. Therefore, a further laboratory determination of the rate constant, including its temperature dependence, stands as one of the important issues critical to improving our understanding on the budget and cycling of Hg. On the other hand, the present model will also benefit from more field studies on the air-surface exchange of Hg^0. These studies will provide much valuable information to modify/correct the assumptions or parameters employed in the model study such as Hg content in surface soil water, etc.

References

Asher, W. E. and Wanninkhof R.: The effect of breaking waves on the analysis of dual-tracer gas exchange measurements, in Air-Water Gas Transfer, Jähne, B. and Monahan, E. C. (Eds.), Aeon Verlag, Hanau, 517–528, 1995.

Bergan, T., Gallardo, L. and Rodhe, H.: Mercury in the global troposphere: a three-dimensional model study, Atmopsh. Env., 33, 1575–1585, 1999.

Bergan, T. and Rodhe, H.: Oxidation of elemental mercury in the atmosphere; Constraints imposed by global scale modelling, J. Atmosph. Chem., 40, 191–212, 2001.

Bidleman, T. F., McConnell, L. L.: Gas exchange of persistent organic pollutants, Science of the Total Environment, 159, 101–117, 1995.

Blanchard, P., Froude, F. A., Martin, J. B., Dryfhout-Clark, H., and Woods, J. H.: Four years of continuous total gaseous mercury (TGM) measurements at sites in Ontario, Canada, At-mopsh. Env., 36, 3735–3743, 2002.

Burke, J., Hoyer, M., Keeler, G., and Scherbatskoy, T.: Wet deposition of mercury and ambient

Title Page

Abstract | Introduction

Conclusions | References

Tables | Figures

◄ | ►

◄ | ►

Back | Close

Full Screen / Esc

Print Version

Interactive Discussion
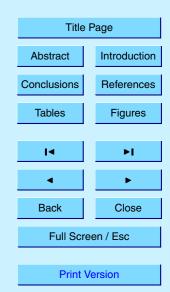
mercury concentration at site in the lake champlain basin, Water, Air & Soil Pollution, 80, 353–362, 1995.

Bullock, O.R. Jr., Benjey W. G. and Keating, M. H.: The modeling of regional-scale atmospheric mercury transport and deposition using RELMAP, in Atmospheric Deposition of Contaminants to the Great Lakes and Coastal Waters, (Ed) Joel E. Baker, pp. 323-347, SETAC Press, Pensacola, 1997.

Bullock, O. R. Jr.: Modeling assessment of transport and deposition patterns of anthropogenic mercury air emissions in the United states and Canada, Science of the Total Environment, 259, 145–157, 2000.

Bullock, O. R. Jr. and Brehme K. A.: Atmospheric mercury simulation using the CMAQ model: formulation description and analysis of wet deposition results, Atmopsh. Env., 36, 2135–2146, 2002.

Byun, D. W. and Ching, J. K. S.: Science algorithms of the EPA models-3 community multi-scale air quality (CMAQ) modeling system, EPA-600/R-99-030 , US Environmental Protection Agency, 1999.

Calhoun, J. A. and Prestbo, E.: Kinetic study of the gas phase oxidation of elemental mercury by molecular chlorine. Report available from Frontier Geosciences inc., 414 Pontius Avenue N., Seattle, WA 98109, 2001.

Carpi A. and Lindberg, S. E.: Application of a Teflon dynamic flux chamber for quantifying soil mercury flux:tests and results over background soil, Atmopsh. Env., 32, 873-882, 1998.

Chang, J. S., Jin, S., Li, Y., Beauharnois, M., Chang, K.-H., Huang, H.-C., Lu, C.-H., Wojcik G., Tanrikulu, S., and DaMassa, J.: The SARMAP air quality model. Part I of SAQM final report, California Air resources Board, Sacramento, CA, 1996.

Fitzgerald, W. F., Vandal, G. M., and Mason, R. P.: Atmospheric cycling and air-water exchange of Hg over mid-continental lacustrine regions. Water, Air & Soil Pollution, 56, 745–767, 1991.

Fitzgerald, W. F., Engstrom D. R., Mason, R. P., and Nater E. A.: The case for atmospheric mercury contamination in remote areas. Environmental Science and Technology, 32, 1, 1–7, 1998.

Gardfeldt, K., Sommar, J., Stromberg, D., and Feng, X.: Oxidation of atomic mercury by hydroxyl radicals and photoinduced decomposition of methylmercury in the aqueous phase, Atmopsh. Env., 35, 3039–3047, 2001.

Hall, B.: The gas phase oxidation of elemental mercury by ozone, Water, Air & Soil Pollution, 80, 301–315, 1995.

Title Page

Abstract | Introduction

Conclusions | References

Tables | Figures

◄ | ►|

◄ | ►

Back | Close
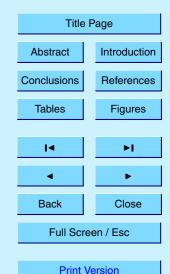
Full Screen / Esc

Print Version

Interactive Discussion

© EGU 2003

Hedley, M., McLaren, R., Jiang, W., and Singleton, D. L.: Evaluation of the MC2-CALGRID photochemical modeling system, National Research Council Canada, Report PET-1361-95S, 1995.

Hornbuckle, K. C., Jeremiason, J. D., Sweet, C. W., and Eisenreich, S. J.: Seasonal variations in air-water exchange of polychlorinated biphenyls in Lake superior, Environ. Sc. Tech., 28, 1491–1501, 1994.

Kim, J. P. and Fitzgerald, W. F.: Sea-air partitioning of mercury in the equatorial Pacific Ocean. Science, 231, 311–330, 1986.

Lin, C. and Pehkonen, S.: Oxidation of elemental mercury by aqueous chlorine (HOCL/OCL$^-$): Implications for tropospheric mercury chemistry, J. Geophys. Res., 103, 28093–28102, 1998.

Lin, C. and Pehkonen, S.: The chemistry of atmospheric mercury: a review, Atmopsh. Env., 33, 2067–2079, 1999.

Lindberg, S. E. and Stratton, W. J.: Atmospheric mercury speciation and behavior of reactive gaseous mercury in ambient air, Environmental Science and Technology, 21, 49–57, 1998.

Lindberg, S. E., Hanson, P. J., Meyers, T. P., and Kim, K. H.: Air/surface exchange mercury vapor over forests – The need for a reassessment of continental biogenic emissions, Atmopsh. Env., 32, 895–908, 1998.

Lindberg, S. and Vermette, S.: Workshop on sampling mercury in precipitation for the National Atmospheric Deposition Program, Atmopsh. Env., 29, 1219–1220, 1995.

Liss, P. S. and Slater, P. G.: Flux of gases across the air-sea interface, Nature, 247, 181–184, 1974.

Mackay, D. and Yeun A. T. K.: Mass transfer coefficient correlations for volatilization of organic solutes from water, Environmental Science and Technology, 17, 211–217, 1983.

Mason, R. P., Fitzgerald, W. F., and Morel, F. M.: The biogeochemical cycling of elemental mercury: anthropogenic influences, Geochemica, 58, 3191–3198, 1994.

Monteith, J. L. and Unsworth, M. H.: Principles of environmental physics, Butterworth-Heinemann (Ed.), 1990.

Munthe J.: The aqueous oxidation of elemental mercury by ozone, Atmopsh. Env., 26A, 1461–1468, 1992.

Pehkonen, S. and Lin, C.: Aqueous photochemistry of mercury with organic acid, J. Air and Waste Management Assoc., 48, 144–150, 1998.

Petersen G., Iverfeldt, A., and Munthe, J.: Atmospheric mercury species over central and north-

A numerical modelling study on regional mercury budget

X. Lin and Y. Tao

ern Europe. Model calculations and comparison with observations from the Nordic air and precipitation network for 1987 and 1988, Atmopsh. Env., 29, 47–67, 1995.

Petersen G., Munthe, J., Pleijel, K., Bloxam, R., and Vinod Kumar, A.: A comprehensive Eulerian modeling framework for airborne mercury species: Development and testing of the tropospheric chemistry module (TCM), Atmosh. Env., 32, 829–843, 1998.

Petersen G., Bloxam, R., Wong, S., Munthe, J., Kruger, O., Schmolke, S. R., and Vinod Kumar, A.: A comprehensive Eulerian modeling framework for airborne mercury species: Model development and application in Europe, Atmosh. Env., 35, 3026–3074, 2001.

Poissant, L. and, M.and Casimir A.: Water-air and soil-air exchange rate of total gaseous mercury measured at background sites, Atmosh. Env., 32, 883-893, 1998.

Poissant, L., Amyot, M., Pilote, M., and Lean, D.: Mercury water – Air exchange over the upper St. Lawrence River and Lake Ontario, Environmental Science and Technology, 34, 3069–3078, 2000.

Ryaboshapko, A., Bullock, O. R., Ebinghaus, R., Ilyin, I., Lohman, K., and Munthe, J., Petersen, G., Seigneur, C., and Wangberg, I.: Comparison of mercury chemistry models, Atmopsh. Env., 36, 3881–3898, 2002.

Seigneur, C., Jwrobel, J., and Constantinou, E.: A chemical kinetic mechanism for atmospheric inorganic mercury, Environmental Science and Technology, 28, 1589–1597, 1994.

Seigneur, C., Abeck, H., Chia, G., Reinhard, M., Bloom, N. S., Prestbo, E., and Saxena P.: Mercury adsorption to elemental carbon (soot) particles and atmospheric particulate matter, Atmopsh. Env., 32, 2649–2657, 1998.
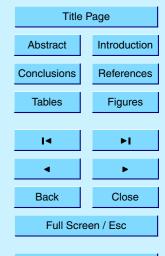
Seigneur C., Karamchandani, P., Lohman, K., and Vijayaraghavan, K.: Multiscal modeling of the atmospheric fate and transport of mercury, J. Geophys. Res., 106, D21, 27795–27809, 2001.

Shannon, J. D. and Voldner, E. C.: Modeling atmospheric concentrations of mercury and deposition to the great lakes, Atmopsh. Env., 29, 1649–1661, 1995.

Smith, R. M. and Martell, A. E.: Critical Stability Constants, vol. 4: Inorganic Complexes, Plenum Press, New York, 1976.

Sommar, J., Gardfeldt, K., Stromberg, D., and Feng, X.: A kinetic study of the gas-phase reaction between the hydroxyl radical and atmoic mercury, Atmopsh. Env., 35, 3049–3054, 2001.

Thibodeaux, J. L.: Environmental chemodynamics: Movement of chemicals in air, water and soil, (Eds.) John wileys & sons, inc., ISBN: 0-471-61295-2, 1996.

Travnikov, O. and Ryaboshapko, A.: Modeling of mercury hemispheric transport and deposition, meteorological Synthesizing Centre – East Report, June 2002.

U.S. EPA: Mercury Study Report to Congress, Volume I: Executive Summary, Report number EPA-452/R-97-003; Volume II: An Inventory of Anthropogenic Mercury Emissions in the United States, Report number EPA-452/R-97-004, 1997.

Van Loon, L., Mader, E. and Scott, S. L.: Reduction of the aqueous mercuric ion by Sulfite: UV spctrum of $HgSO_3$ and its intramolecular redox reaction, J. Phys. Chem., 104, 1621–1626, 2000.

Wanninkhof, R., Ledwell, R. Jr., and Broecker, W. S.: Gas exchange – wind speed relationship measured with sulfur hexafluoride on a lake, Science, 227, 1224–1226, 1985.

Xu, X., Yang, X., Miller, D. R., Helble, J. J., and Carley, R. J.: Formulation of bi-directional atmosphere-surface exchanges of elemental mercury, Atmopsh. Env., 33, 4345–4355, 1999.

Xu, X., Yang, X., Miller, D. R., Helble, J. J., and Carley, R. J.: A regional scale modeling study of atmospheric transport and transformation of mercury, II. Simulation results fot the northeast United States, Atmopsh. Env., 34, 4945–4955, 2000.

Title Page

Abstract | Introduction

Conclusions | References

Tables | Figures

◄ | ►

◄ | ►

Back | Close

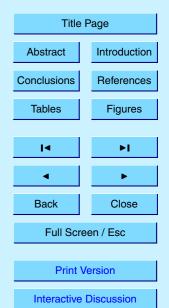Full Screen / Esc

Print Version

Interactive Discussion

Table 1. The physio-chemical transformation mechanism of Hg integrated into CMAQ and associated rate constants

Reaction (Process)		Constants	Reference
Gas-phase Chemistry			
$Hg^0_{(g)} + Cl_{2(g)}$	$\rightarrow RGM_{(g)}$	$4.8 \times 10^{-18} \ cm^3 molec^{-1}s^{-1}$	Calhoun and Prestbo (2001)
$Hg^0_{(g)} + O_{3(g)}$	$\rightarrow .5RGM_{(g)}+.5HgP_{(insoluble)}$	$3.0 \times 10^{-20} \ cm^3 molec^{-1}s^{-1}$	Hall (1995)
$Hg^0_{(g)} + H_2O_{2(g)}$	$\rightarrow RGM_{(g)}$	$8.5 \times 10^{-19} \ cm^3 molec^{-1}s^{-1}$	Tokos et al. (1998)
$Hg^0_{(g)} + OH_{(g)}$	$\rightarrow .5RGM_{(g)}+.5HgP_{(insoluble)}$	$2.9 \times 10^{-14} \ cm^3 molec^{-1}s^{-1}$	see text
Gas-Droplet Equiliblia			
$Hg^0_{(g)}$ $\Leftrightarrow$	$Hg^0_{(aq)}$	$1.1 \times 10^{-1} M \ atm^{-1}$	Seigneur et al. (1994)
$RGM_{(g)}$ $\Leftrightarrow$	$RGM_{(aq)}$	$1.4 \times 10^{+6} \ M \ atm^{-1}$	Seigneur et al. (1994)
$Cl_{2(g)}$ $\Leftrightarrow$	$Cl_{2(aq)}$	$7.6 \times 10^{-2} \ M \ atm^{-1}$	Lin and Pehkonen (1998)
Ionic Equilibria in Aqueous Phase			
$Hg^{2+} + SO_3^{2-}$ $\Leftrightarrow$	$HgSO_3$	$2.0 \times 10^{-13} \ M$	Smith and Martell (1976)
$HgSO_3 + SO_3^{2-}$ $\Leftrightarrow$	$Hg(SO_3)_2^{2-}$	$4.0 \times 10^{-12} \ M$	Smith and Martell (1976)
$Hg^{2+} + 2Cl^-$ $\Leftrightarrow$	$HgCl_2$	$1.0 \times 10^{-14} \ M^2$	Lin and Pehkonen (1999)
$Hg^{2+} + OH^-$ $\Leftrightarrow$	$HgOH^+$	$2.51 \times 10^{-11} \ M$	Smith and Martell (1976)
$HgOH^+ + OH^-$ $\Leftrightarrow$	$Hg(OH)_2$	$6.31 \times 10^{-12} \ M$	Smith and Martell (1976)
$HgOH^+ + Cl^-$ $\Leftrightarrow$	$HgOHCl$	$3.72 \times 10^{-8} \ M$	Smith and Martell (1976)
Chlorine Reactions in Aqueous Phase			
$Cl_{2(aq)} + H_2O$ $\Leftrightarrow$	$HOCl + Cl^- + H^+$	$k = 10^{-3.3}$	Lin and Pehkonen (1998)
$HOCl$ $\Leftrightarrow$	$OCl^- + H^+$	$k = 10^{-7.5}$	Lin and Pehkonen (1998)
Hg Oxidation in Aqueous Phase			
$Hg^0_{(aq)} + O_{3(aq)} \rightarrow Hg^{2+}_{(aq)} + products$		$4.7 \times 10^7 \ M^{-1}s^{-1}$	Munthe (1992)
$Hg^0_{(aq)} + {}^\cdot OH_{(aq)} \rightarrow Hg^{2+}_{(aq)} + Products$		$2.4 \times 10^9 \ M^{-1}s^{-1}$	Gardfeldt et al. (2001)
$Hg^0_{(aq)} + HOCL_{(aq)} \rightarrow Hg2^+_{(aq)} + Cl^-_{(aq)} + OH^-_{(aq)}$		$2.09 \times 10^6 \ M^{-1}s^{-1}$	Lin and Pehkonen (1998)
$Hg^+_{(aq)} + OCL^-_{(aq)} \rightarrow Hg^{2+}_{(aq)} + OH^-_{(aq)}$		$1.99 \times 10^6 \ M^{-1}s^{-1}$	Lin and Pehkonen (1998)
Hg Reduction in Aqueous Phase			
$HgSO_{3(aq)}$	$\rightarrow Hg^0_{(aq)} + Products$	$T \cdot e^{31.971-12595/T} \ s^{-1}$	Van Loon et al. (2000)
$Hg(OH)_{2(aq)} + h\nu$	$\rightarrow Hg^0_{(aq)} + Products$	$6.0 \times 10^{-7} \ s^{-1}$ (Maximum)	Bullock and Brehme (2002)
$Hg^{2+}_{(aq)} + {}^\cdot HO_2$	$\rightarrow Hg^0_{(aq)} + Products$	$1.1 \times 10^4 \ M^{-1}s^{-1}$	Pehkonen and Lin (1998)
Sorption Equilibrium in Aqueous Phase			
$RGM_{(aq)} + ATM$ $\Leftrightarrow$	$HgP_{(soluble)}$	$k=34 \ Lg^{-1}$; $ATM=0.02 \ gL^{-1}$	Seigneur et al. (2001)

Table 2. Comparisons of modelled total wet deposition of Hg and averaged ground level concentration of TGM over the four-week modeling period with measurements

Wet Deposition of Hg over 20/06/1995 - 18/07/1995			Ground Level Concentration of TGM Averaged over 20/06/1995 - 18/07/1995		
MDN Obs. Site	Obs. Value (ng m^{-2})	Model Value (ng m^{-2})	Obs. Site	Obs. Value (ng m^{-3})	Modelled Value (ng m^{-3})
DE02	1044	1335.2	Egbert, ON (Blanchard et al., 2002)	1.8	1.80
KY99	994	981.9	Burnt Island, ON (Blanchard et al., 2002)	1.7	1.76
NC08	1538	2225.7	Point Petre, ON (Blanchard et al., 2002)	2.0	1.80
NY97	2120	2097.2	Underhill, VT (Burke et al., 1995)	1.9	1.71
SC19	2129	2433.1	Trout Lake, WI (Fitzgerald et al., 1991)	1.6	1.66
WI36	1754	1292.0	Walker Branch Watershed, TN (Lindberg and Stratton, 1998)	2.2	1.88

Title Page

Abstract Introduction

Conclusions References

Tables Figures

◄◄ ►►

◄ ►

Back Close

Full Screen / Esc

Print Version

Interactive Discussion

© EGU 2003

Table 3. Comparisons of modelled weekly wet deposition of Hg with measurements from 11 MDN sites

MDN Observation Site	06/20 – 06/27		06/27 – 07/04		07/04 – 07/11		07/11 – 07/18	
	Obs (ng m^{-2})	Model (ng m^{-2})	Obs (ng m^{-2})	Model (ng m^{-2})	Obs (ng m^{-2})	Model (ng m^{-2})	Obs (ng m^{-2})	Model (ng m^{-2})
DE02	40	179.6	646	64.5	0	0.0	358	1091.1
IL11	N/A		95	380.9	N/A		N/A	
KY99	36	577.2	425	0.0	533	0.0	0	404.7
MN16	378	104.6	222	360.5	371	591.4	N/A	
MN18	N/A		347	510.9	182	317.4	N/A	
NC08	130	293.6	286	473.0	548	388.2	574	1070.8
NC42	1207[*]	846.8	N/A		493[**]	204.8	N/A	
NY97	761	623.1	16	403.2	650	589.9	693	481.1
SC19	972	1143.9	250	878.3	697	410.8	210	0.0
WI08	161	0.3	383	432.1	207	224.5	N/A	
WI36	234	366.0	0	29.7	227	234.2	1293	662.1

* Sample dates 06-22-1995 to 06-29-1995
** Sample dates 07-06-1995 to 07-13-1995

A numerical modelling study on regional mercury budget

X. Lin and Y. Tao

Title Page

Abstract · Introduction

Conclusions · References

Tables · Figures

◄◄ · ►►

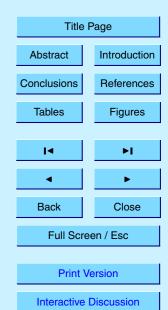◄ · ►

Back · Close

Full Screen / Esc

Print Version

Interactive Discussion

© EGU 2003

Table 4. Comparison of statistics among MDN measurements, results of Bullock and Brehme (2002), results from baseline run and results from sensitivity test run (see text for detail)

Sample #	Data Source	Mean (ng m^{-2})	σ	Min. (ng m^{-2})	Percentile (ng m^{-2})			Max. (ng m^{-2})
					25th	50th	75th	
35	MDN Measurement	389.3	327.3	0.0	171.5	347.0	561.0	1293.0
35	Bullock and Brehme (2002)	623.7	621.1	0.0	202.1	482.5	759.7	2598.5
35	Baseline Run	409.7	318.9	0.0	192.2	388.2	583.5	1143.9

A numerical modelling study on regional mercury budget

X. Lin and Y. Tao

Table 5. Domain total deposition of Hg calculated over the period of 20 June 1995 to 18 July 1995 from four scenario runs

Scenarios	Emis. within Domain (Kg)	Dry Deposition over Entire Domain (Kg) *(Bracketed values refer to differences from the Background Scenario S_b)*			Wet Deposition over Entire Domain (Kg) *(Bracketed values refer to differences from the Background Scenario S_b)*		
		Hg^0	RGM	HgP	Hg^0	RGM	HgP
S_0: Base Line	20697.2	6068.2	4276.8	158.5	1.2	3683.4	6048.0
		10503.4 *(2230.4)*			9732.6 *(1528.6)*		
		20236.0 *(3759.0)*					
S_{ba}: Background+ Anth. Emis.	8216.4	5637.4	4192.0	155.4	1.2	3612.0	5940.3
		9984.7 *(1711.7)*			9553.5 *(1349.5)*		
		19538.2 *(3061.2)*					
S_{bn}: Background+ Re-Emis.	12480.9	5920.9	2751.3	124.6	1.2	3154.6	5228.4
		8796.8 *(523.8)*			8384.3 *(180.3)*		
		17181.0 *(704.0)*					
S_b: Background Only		5485.4	2666.2	121.5	1.2	3082.5	5120.3
		8273.0			8204.0		
		16477.0					

Table 6. Statistics comparison between baseline run and sensitivity test run

	Bias $(ng\ m^{-2})$	Error $(ng\ m^{-2})$	Relative Bias	Relative Error	RMSE $(ng\ m^{-2})$	Index of Agreement
Baseline (S_0) Run	20.4	267.2	1.51	2.02	331.5	0.6745
Sensitivity Test Run	262.5	399.6	2.97	3.33	518.0	0.5996

Fig. 1. The model domain. Also shown are the site locations of measurements used to evaluate the model performance (see text for details).

A numerical modelling study on regional mercury budget

X. Lin and Y. Tao

Title Page

Abstract | Introduction

Conclusions | References

Tables | Figures

◀ | ▶

◀ | ▶

Back | Close

Full Screen / Esc

Print Version

Interactive Discussion

Fig. 2. Total re-emissions of Hg^0 (ng m^{-2}) from natural surfaces over the period of 20 June 1995 to 18 July 1995.

Title Page

Abstract | Introduction

Conclusions | References

Tables | Figures

◀ | ▶

◀ | ▶

Back | Close

Full Screen / Esc

Print Version

Interactive Discussion

Fig. 3. Calculated total wet deposition of Hg (ng m^{-2}) over the period of 20 June 1995 to 18 July 1995.

Fig. 4. Total precipitation (cm) over the period of 20 June 1995 to 18 July 1995, as inputted to CCTM.

Fig. 5. Total anthropogenic emissions of RGM and HgP (ng m^{-2}) over the period of 20 June 1995 to 18 July 1995, as inputted to CCTM.

A numerical modelling study on regional mercury budget

X. Lin and Y. Tao

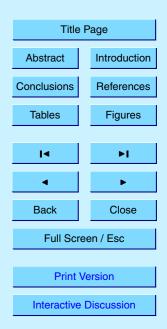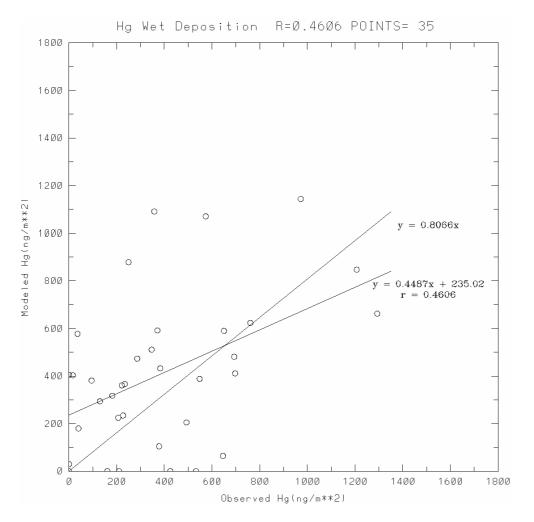**Fig. 6.** Scatter plot of modelled versus measured wet deposition of Hg. Also shown are a least-squares regression line and a forced regression line with zero intercept.